Metaplastic Changes of Nasal Respiratory Epithelium in Rats Exposed to Hexamethylphosphoramide (HMPA) by Inhalation

K. P. LEE, DVM, PhD,
and H. J. TROCHIMOWICZ, ScD

From the Haskell Laboratory for Toxicology and Industrial Medicine,
E. I. du Pont de Nemours and Company, Inc., Newark, Delaware

Rats exposed by inhalation to hexamethylphosphoramide (HMPA) at concentrations of 50, 100, 400, and 4000 parts per billion (ppb) for 6–24 months revealed nasal tumors and squamous metaplasia with inflammation in the nasal epithelium, but no changes were observed at 10 ppb. The ciliated cells were most susceptible to HMPA, showing degenerative changes, with abnormal cilia and extensive deciliation. The desquamated nasal epithelium was repaired initially by undifferentiated mucus or microvillous cuboidal cells, and subsequently the lining cells were replaced with squamous cells migrating upward from the basal layer. In the early stage of squamous metaplasia, thickened nasal epithelium revealed indifferent cells, undifferentiated glandular cells, transitional cells from glandular to squamous cells, poorly differentiated squamous cells, and intermediate cells showing features of glandular and squamous differentiation. Subsequently, the undifferentiated glandular cells were replaced mainly with the squamous or intermediate cells. The undifferentiated glandular cells appeared to be biphasic reserve cells capable of differentiating to glandular or squamous cells. The intermediate cells appeared to be derived from the undifferentiated glandular cells and converted into keratinizing squamous cells. Numerous secretory vesicles and mucus droplets were observed in the squamous cells adjacent to the keratinized area and keratin plates. (Am J Pathol 1982, 106:8–19)

BECAUSE HEXAMETHYLPHOSPHORAMIDE (HMPA) is a powerful organic solvent and has low acute toxicity, it has been extensively used in research laboratories and plastic industries.[1] It has also been widely tested as a chemosterilant for insects and other organisms.[2-5] The toxic effects of oral administration were degeneration in the renal tubules,[6] bronchopneumonia,[7] and testicular atrophy.[8] Oral administration of HMPA showed synergistic effects on *Mycoplasma pulmonis* and enhanced the incidence of murine pneumonia and rhinitis.[9] Nasal tumors developed in the rats exposed to HMPA by inhalation at concentrations of 4000, 400, 100, and 50 parts per billion (ppb) for 7–24 months.[10,11]

Nasal tumors related to occupational exposure have been reported in workers in the furniture industry,[12,13] shoe industry,[14,15] and nickel refineries.[16,17] Formaldehyde,[18] bis(chloromethyl)ether,[19] chloromethyl methyl ether,[20] and other industrial chemicals[21-24] are known to cause nasal tumors in experimental animals. In spite of the fact that man has been exposed to some of these chemicals by occupational exposure for many years, there are no epidemiologic studies indicating carcinogenicity in the nasal cavity of man. Few reports concerning ultrastructural studies on the normal and abnormal mucosa of the rats are available, although rats have been used extensively for many years in inhalation toxicity studies. This investigation was conducted to elucidate the ultrastructural alterations of the nasal respiratory epithelium exposed to HMPA, with emphasis on the pathogenesis of preneoplastic squamous metaplasia.

Materials and Methods

Experimental Design

Experiment 1

A total of 960 Charles-CD Sprague-Dawley-derived male and female rats was divided into eight

equal groups of 120 males and 120 females. Group 1 male and group 2 female rats were exposed to air and served as controls. Sixty of the 120 males (Group 3) and 60 of the 120 females (Group 4) were exposed to HMPA at a concentration of 50 ppb (parts per billion) for 1 year and were placed in the holding rooms. The remaining 60 males and 60 females were exposed continuously for 2 years. Group 5 males and Group 6 females were exposed at a concentration of 400 ppb for 10 months. Group 7 males and Group 8 females were exposed at a concentration of 4000 ppb for 9 months. After 3 months' exposure necropsy was performed on 18 rats from each group. At 8 months' exposure, 6 rats were sacrificed, respectively, in Group 3 male and Group 4 female rats. After 1 year of exposure 20 rats in Groups 3 and 4 were sacrificed with 20 rats from control Groups 1 and 2. Remaining rats in all groups were sacrified after two years exposure.

Experiment 2

A total of 800 Charles-CD Sprague–Dawley-derived male and female rats was divided into eight equal groups of 100 males and 100 females. Group 1-A males and Group 2-A females were exposed to air and used as controls. Group 3-A male and group 4-A female rats were exposed to HMPA at 50 ppb. Group 9 male and Group 10 female rats were exposed to HMPA at a concentration of 10 ppb for 2 years. Fifty of the 100 males (Group 11) and 50 of the 100 female rats (Group 12) were exposed to HMPA at a concentration of 100 ppb for 6 months. The remaining 50 males and 50 females were exposed continuously for 13 months. Twenty rats in Group 3-A male and 4-A females were sacrificed after 1 year of exposure. All rats were sacrificed at the end of 2 years' exposure and subjected to microscopic examination, except Group 3-A male and group 4-A female rats. The lung, trachea, thyroid, pituitary, adrenal, testis, and kidney were fixed in Bouin's solution, and all remaining organs and tissues were fixed in 10% formalin solution. After the nose was fixed in Bouin's solution and decalcified, three coronal sections from the anterior nasal cavity and two coronal sections from the posterior nasal cavity were prepared for light-microscopic examination. The sections were stained with hematoxylin and eosin, periodic acid–Schiff (PAS), alcian blue, and modified trichrome stain. The nasoturbinates and nasal septum of 1 male and 1 female rat from each group at different sacrifice periods were subjected to electron-microscopic examination. For electron-microscopic examination, the excised tissues were fixed in 3% glutaraldehyde for approximately 1 hour. They were then rinsed in Millonig's phosphate buffer, postfixed for 2 hours at 4 C

in 1% osmium tetroxide, dehydrated in alcohol, and embedded in Epon. Sections (1 μ thick), stained with toluidine blue, were utilized in locating areas for electron-microscopic examination.

Results

Light Microscopy

The incidence and severity of the rhinitis, squamous metaplasia of the nasal epithelium, and nasal tumors showed a definite dose-response in the rats at 50, 100, 400, and 4000 ppb, but no changes were found at 10 ppb (Table 1). Most nasal tumors occurred in the respiratory epithelium of the anterior nasal cavity and invaded ventral nasal bone or the posterior nasal cavity. The primary tumor of olfactory epithelium in the ethmoturbinates was relatively rare. Early stage tumor development was often found in the respiratory epithelium of nasoturbinates, nasal septum, or olfactory epithelium of the ventral nasal cavity, but less often in the respiratory epithelium of maxilloturbinates. Most of the nasal tumors were squamous cell carcinomas (Figures 2, 6, 7, and 8) that had developed from metaplastic epithelium (Figure 1) or subepithelial nasal gland (Figure 5). Adenoid squamous cell carcinomas (Figure 4) were also formed from metaplastic respiratory epithelium (Figure 7), subepithelial gland, and Stenson's gland, (Figure 3) located adjacent to the maxillary sinus. In early stages of squamous metaplasia, hyperplastic cellular aggregates were observed in the basal cell layer. The respiratory epithelium became markedly thickened by stratification of columnar and cuboidal cells without hyperkeratosis (Figures 10 and 11). Subsequently, the epithelium was replaced with flattened squamous epithelium with hyperkeratosis. PAS-alcian-blue–positive material was observed in the metaplastic cells, and the intensity of the staining was markedly decreased in the keratinized squamous epithelium (Figure 1). The metaplastic lesions of nasal gland integrated into the squamous metaplasia that had developed from the respiratory epithelium and formed large metaplastic lesions.

Electron Microscopy

The ciliated cells revealed denudation of the cilia and abnormal compound cilia showing several to more than 12 axial filament complexes (Figure 9). The compound cilia were enclosed within the cytoplasmic projections. Degenerating ciliated cells (Figure 9) exhibited mitochondrial swelling, focal disruption of cytoplasmic membrane, and cystic dilatation of the cisternae in rough endoplasmic
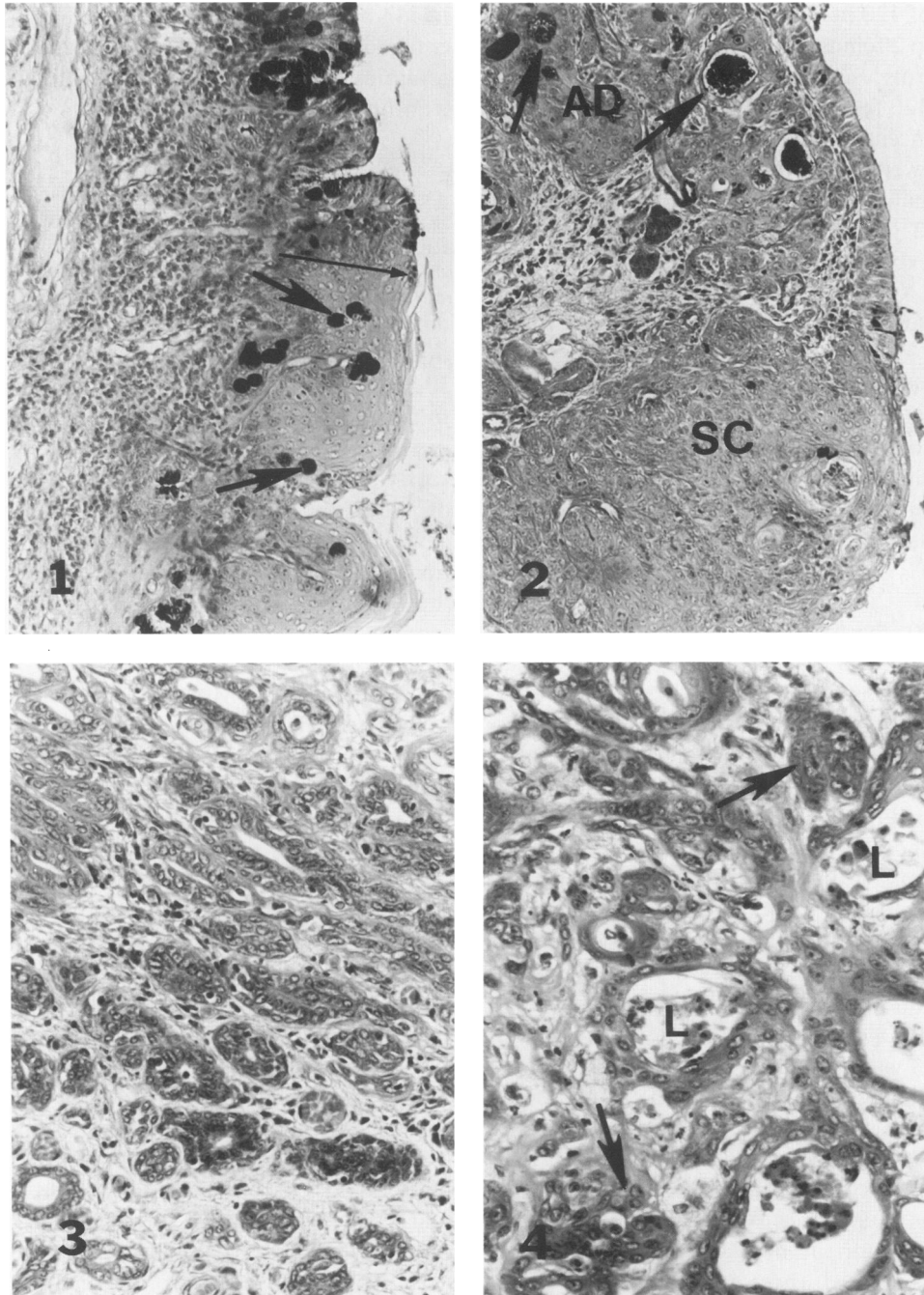
Figure 1—Squamous metaplastic epithelium of the nasal septum shows PAS-positive material (*arrows*). Note tiny PAS-positive droplets (*slender arrow*) in the keratinized layer of squamous metaplasia. (PAS, × 100)   **Figure 2**—Nasoturbinate reveals squamous cell carcinoma (*SC*) in the respiratory epithelium and adenoid squamous cell carcinoma (*AD*) in the subepithelial gland showing PAS-positive material (*arrows*). Note intact respiratory epithelium adjacent to the adenoid squamous cell carcinoma. (PAS, × 100)   **Figure 3**—Hyperplastic Stenson's gland located adjacent to the maxillary sinus shows squamous metaplasia. (H&E, × 250)   **Figure 4**—Adenoid squamous cell carcinoma shows both glandular and squamous structure. The lumen (*L*) of glandular acini replaced by squamous cells shows desquamated epithelial cells, homogenous eosinophilic material, and cellular debris. Some glandular acini are obliterated by squamous cells (*arrows*). (H&E, × 250)

reticulum (RER). Similarly, the goblet cells showed sloughing microvilli, cytoplasmic disruption, and large lakes of RER cisternae containing electron-lucent granules. When degenerating ciliated and mucus cells were sloughed, the epithelium was in-

itially repaired by poorly differentiated mucus cells (Figure 10) showing scanty mucus droplets or cuboidal cells (microvillous cells) showing well-developed Golgi complex, RER, and microvilli. Subsequently, the epithelial cells were replaced with

Table 1—Incidence of Squamous Metaplasia and Nasal Tumor in Rats Exposed to HMPA

	Group						
	1,2	1-A, 2-A*	9, 10*	3, 4	11, 12*	5, 6	7, 8
Exposure concentration (ppb)	0	0	10	50	100	400	4000
Number of rats	240	200	200	240	200	240	240
Number of tissue examined	231	194	196	235	196	228	228
Squamous metaplasia	7	12	16	58	112	171	189
	(3.0%)	(6.2%)	(8.2%)	(24.7%)	(57.1%)	(74.7%)	(82.9%)
Number of tissue samples examined	196	200	200	194	200	219	215
Papilloma	0	0	0	9 (4.6%)	6 (3.0%)	13 (5.9%)	11 (5.1%)
Adenomatoid polyp	0	0	0	0	1 (0.5%)	0	0
Epidermoid carcinoma	0	0	0	24 (12.4%)	59 (29.5%)	137 (62.6%)	120 (55.8%)
Adenoid squamous carcinoma	0	0	0	4 (2.1%)	5 (2.5%)	21 (9.6%)	41 (19.1%)
Adenocarcinoma	0	0	0	1 (0.5%)	1 (0.5%)	2 (0.9%)	2 (0.9%)
Transitional carcinoma	0	0	0	1 (0.5%)	1 (0.5%)	3 (1.4%)	4 (1.9%)
Undifferentiated carcinoma	0	0	0	0	2 (1.0%)	2 (0.9%)	1 (0.5%)
Pleomorphic (mixed) tumor	0	0	0	0	0	2 (0.9%)	0
Total tumor/group				39/194 (20.0%)	75/200 (37.5%)	180/219 (82.2%)	179/215 (83.3%)

* Group belongs to second experiment. Groups with odd numbers are males and even numbers, females.

poorly differentiated cuboidal cells showing scanty cellular organelles and microvilli. The ciliated cells were not found in the regenerated epithelial cells. In the stage of squamous cell stratification, the superficial microvillous cells showed cytoplasmic edema, degenerative changes in the cellular organelles, and desquamation. The desquamated microvillous cells were replaced with cuboidal or flattened squamous cells migrating upward. The epithelial surface was covered completely by squamous cells showing either blunt cytoplasmic processes or undulated smooth cytoplasmic membrane. There were undifferentiated cells, poorly differentiated glandular cells, transitional cells from glandular to squamous cells, intermediate cells showing features of glandular and squamous differentiation, and squamous cells on the basal lamina. In some areas, the thickness of epithelium increased markedly by stratification of poorly differentiated glandular cells. Subsequently, the glandular cells were replaced mostly by transitional cells and poorly differentiated squamous cells.

Poorly differentiated glandular cells (Figures 11 and 12) revealed secretory droplets, well-developed Golgi complex, and electron-lucent cytoplasm with numerous lakes of RER containing electron-dense granules. The cells were adjoined with poorly differentiated squamous cells by a few desmosomes. Transitional cells (Figures 12 and 14) from glandular to poorly differentiated squamous cells were characterized by electron-lucent cytoplasm, parallel hyperplastic RER, dilated cisternae of RER with electron-dense granules, interdigitated cytoplasmic processes, and a few desmosomes. Poorly differentiated squamous cells (Figure 11) showed electron-dense cytoplasm, scanty tonofibrils, and short cytoplasmic processes with a few desmosomes, while differentiated squamous cells were characterized by electron-dense cytoplasm, abundant tonofibrils, glycogen particles, and markedly interdigitated cytoplasmic processes with numerous desmosomes. The intermediated cells (Figure 13) showed scanty tonofibrils, well-developed RER, dilated RER cisternae, secretory vesicles or droplets, interdigitated cytoplasmic processes, and desmosomes. The indifferent cells were larger than the basal cells and had light cytoplasmic density with scanty cellular organelles. The basal cells were small and contained electron-dense cytoplasm and relatively scanty cellular organelles. Slightly interdigitated cytoplasmic processes of the basal cells were adjoined with cells by poorly developed desmosomes.

In the later stages of nonkeratinized squamous metaplasia, unlike the basal cells seen in the normal or early stage of squamous metaplasia, the basal cells transformed into more distinctively squamous cells showing tonofibrils, numerous interdigitated processes, and well-developed desmosomes. The epithelium showed mainly stratification of poorly differentiated squamous and intermediate cells. The squamous cells in the basal layer had slightly wider intercellular spaces and fewer tonofibrils and desmosomes than those of the squamous cells in the intermediate layer. The squamous cells in the upper layer were cuboidal or flattened, and the intercellular spaces were narrower than those of the intermediate layer.

The keratinized squamous epithelium revealed the stratum basalis, spinosum, granulosum, and cor-
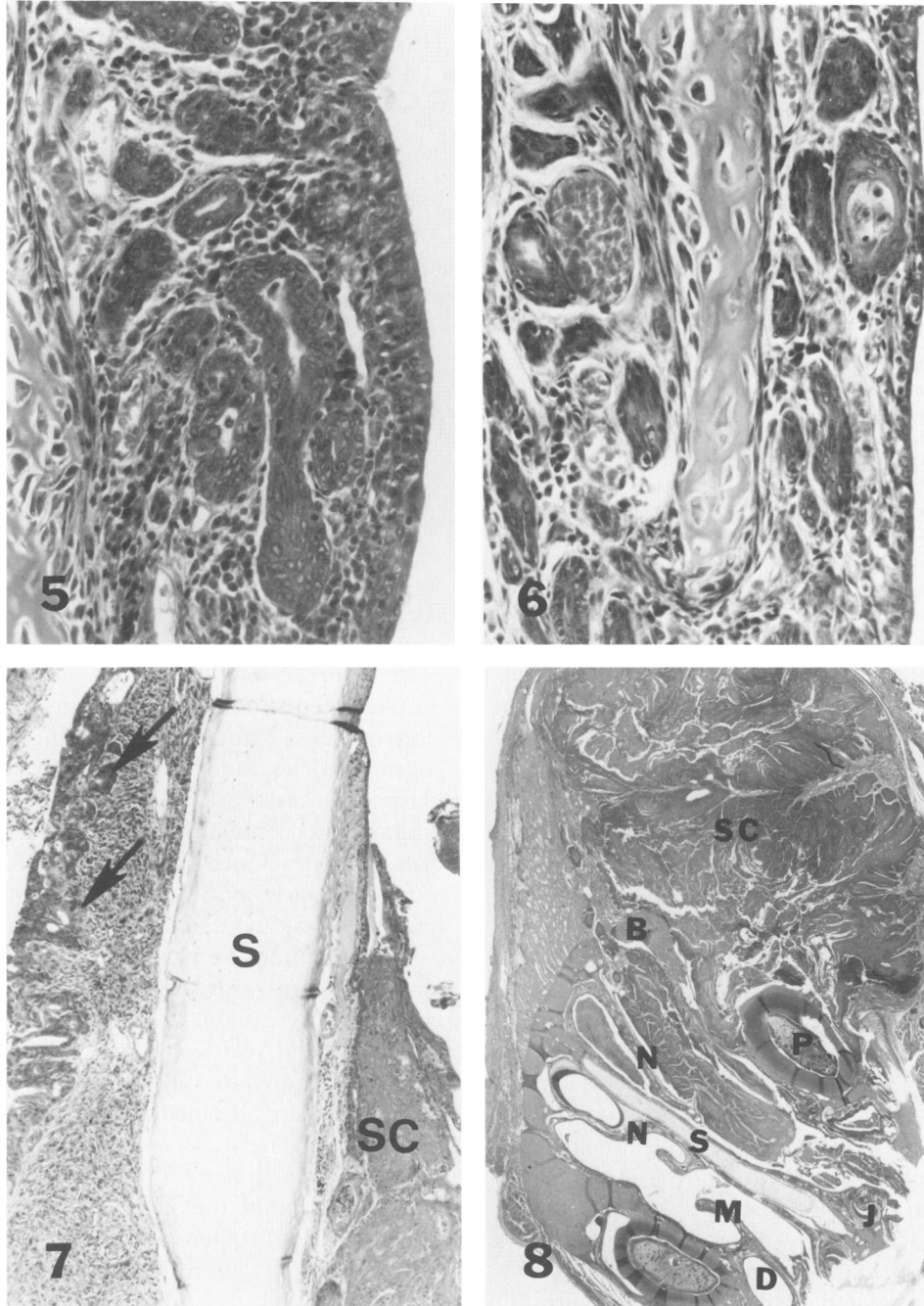
Figure 5—Nasoturbinate shows squamous metaplasia in the respiratory epithelium and subepithelial nasal gland with cellular infiltration. (H&E, ×250)   Figure 6—Nasoturbinate reveals squamous cell carcinoma in the subepithelial nasal gland with thin layer of squamous metaplasia of the respiratory epithelium and inflammatory cell infiltration. (H&E, ×250)   Figure 7—The respiratory epithelium of nasal septum (S) shows glandular dysplasia (arrows) and squamous cell carcinoma (SC). (H&E, ×50)   Figure 8—Right nasal cavity is obliterated by squamous cell carcinoma (SC) showing extensive destruction of the nasal bone (B) and protrusion. N = nasoturbinate; M = maxilloturbinate; S = nasal septum; J = Jacobson's organ; P = pulp of incisor tooth; D = nasolacriminal duct. (H&E, ×6)

neum. The squamous cells contained more tonofibrils than the squamous cells in the stage of nonkeratinized squamous metaplasia. The number of desmosomes, tonofibrils, keratohyaline granules, and membrane-bound granules was increased progressively toward the upper layer in the stratum spinosum and granulosum. The cytoplasm of intermediate cells in the stratum granulosum was packed with numerous secretory droplets and tonofibril bundles (Figure 15). Occasionally numerous vesicles were accumulated in the cytoplasm of nonkeratinized superficial squamous cells. In the stratum corneum, the keratocytes showed
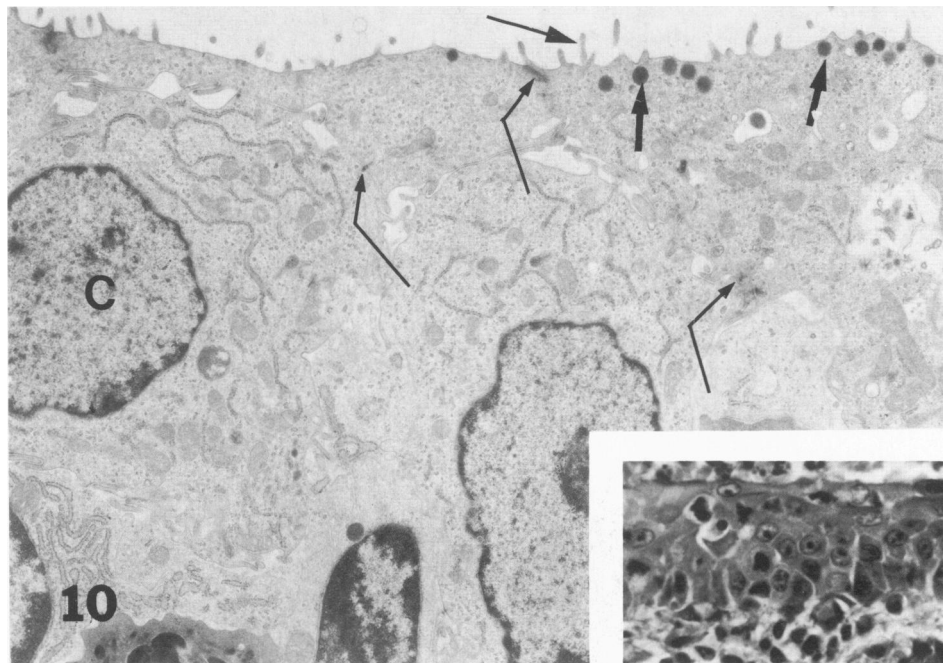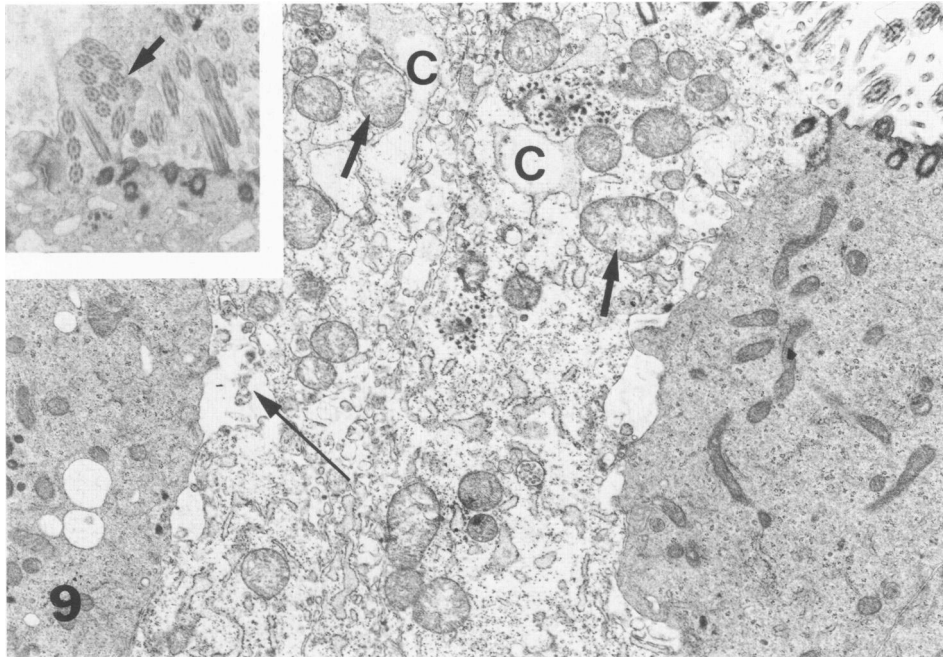
Figure 9—A ciliated epithelial cell shows electron-lucent cytoplasm, mitochondrial swelling with disrupted cristae (*arrow*), cystic dilation of RER cisternae (*C*), and focal disruption of cytoplasmic membrane (*slender arrow*). (× 7800)   **Inset**—A cytoplasmic projection contains compound cilia (*arrow*). (× 7800)   **Figure 10**—An undifferentiated mucus cell reveals several mucus droplets (*short arrows*), microvilli (*slender arrows*), relatively well-developed RER, and junctional complex (*bent arrows*). Note a cuboidal cell (*C*) showing relatively well developed RER, scanty microvilli, and absence of mucus droplets. (× 7800)   **Inset**—Superficial lining cells in early stage of squamous metaplasia are cuboidal in shape, and the free surface of the cytoplasmic membrane is PAS-positive. (PAS method, × 400)

secretory droplets with scanty organelles and glycogen aggregates, and some cornified plates contained numerous secretory droplets (Figure 16).

Discussion

The ciliated cells appeared to be most susceptible to HMPA exposure and showed degenerative changes

with deciliation. The ciliated cells were not seen in the early repair stage of desquamated epithelium with mucus and microvillous cells. Since ciliated cells are normally the end stage of cell differentiation from the basal cells, the destroyed ciliated cells are unable to repopulate because of aberrant cellular differentiation in the metaplastic process. Absence of ciliated
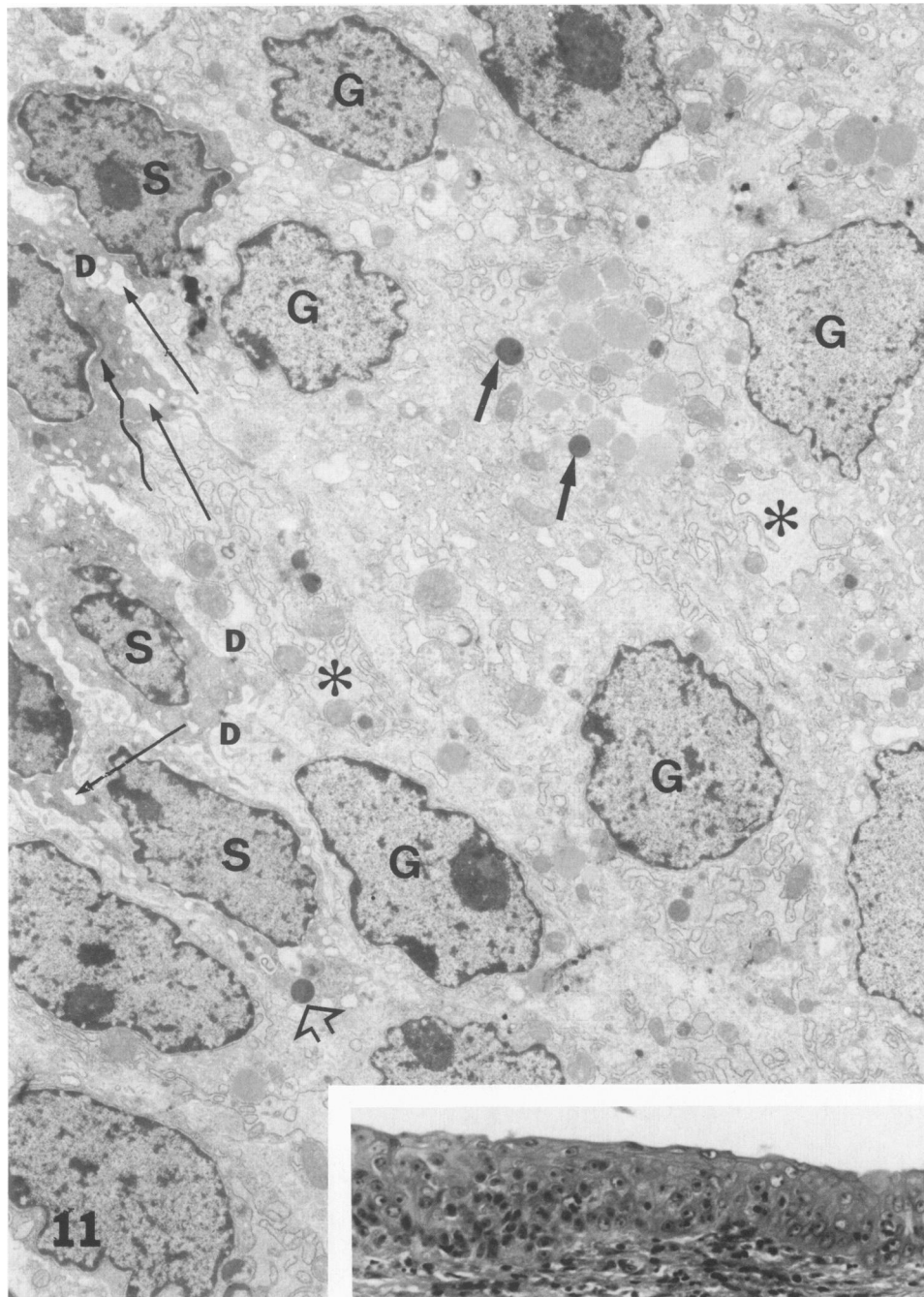
Figure 11—Note stratification of undifferentiated glandular cells (G) and poorly differentiated squamous cells (S). The undifferentiated glandular cells reveal electron-lucent cytoplasm with lakes of RER cisternae (asterisks) and a few secretory droplets (large arrows). The poorly differentiated squamous cells show electron-dense cytoplasm, markedly dilated RER cisternae (slender arrows), scanty tonofibrils (twisted arrow), a few secretory droplets (hollow arrows), and slightly interdigitated cytoplasmic processes with desmosomes (D). (× 5000)   Inset— Nonkeratinized squamous metaplasia shows stratification of columnar and cuboidal cells with lymphocytic infiltration. (H&E stain, × 250)

cells was described in epidermoid nasal carcinoma,[25] carcinoma in situ of the bronchus,[26] carcinoma of the trachea induced by chemical carcinogen,[27] and bronchial epithelium exposed to dust and chemical.[28] In this experiment the most striking finding was

numerous intermediate cells and numerous mucus droplets in the keratin plates of keratinized squamous metaplasia of nasal epithelium. Similar intermediate cells were reported in mucoepidermoid carcinoma,[29-31] epidermoid nasal tumors induced by
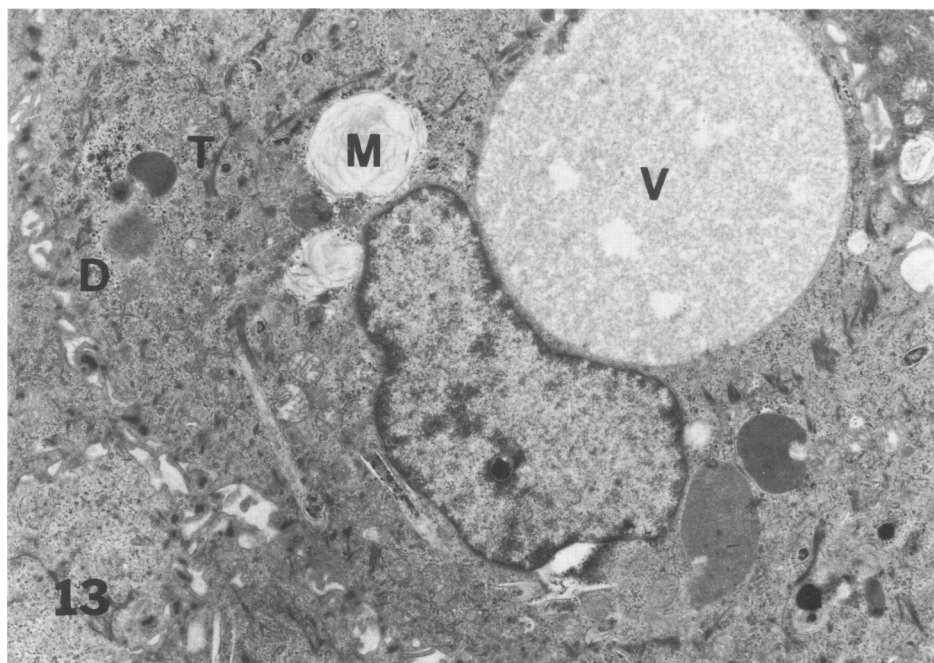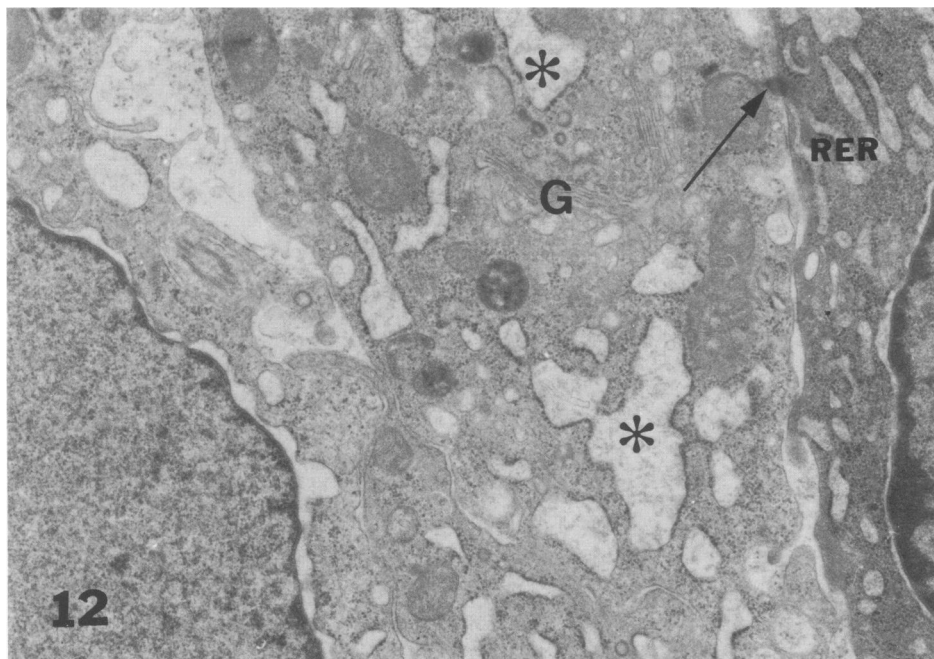
Figure 12—Higher magnification of undifferentiated glandular cell exhibits electron-lucent cytoplasm, Golgi complex (*G*), and lakes of RER cisternae containing electron-dense granules (*asterisks*). The adjoining transitional cell has a tight junction (*slender arrow*), slightly electron-dense cytoplasm, and parallel RER showing dilatated cisternae with electron-dense granules. (× 19,600)   **Figure 13**—Intermediate cell shows mucus droplets (*M*), tonofibrils (*T*), and interdigitated cytoplasmic processes with numerous desmosomes (*D*). Notice the large cystic vesicles (*V*) filled with electron-dense granules. (× 7800)

a chemical carcinogen in hamsters,[25] undifferentiated uterine cancer,[32] the opening of the bronchial gland,[33] and squamous metaplasia of tracheobronchial epithelium of hamsters treated with a carcinogen.[34-36] Focal squamous metaplasia in the opening of the bronchial gland revealed intermediate goblet and squamous cells in a normal dog, rabbits, and swine. The intermediate cells were interpreted as a transformation of goblet cells into squamous cells through a quantitative change of cytoplasmic components, rather than a qualitative change. The source of these altered "squamoid goblet cells" was con-
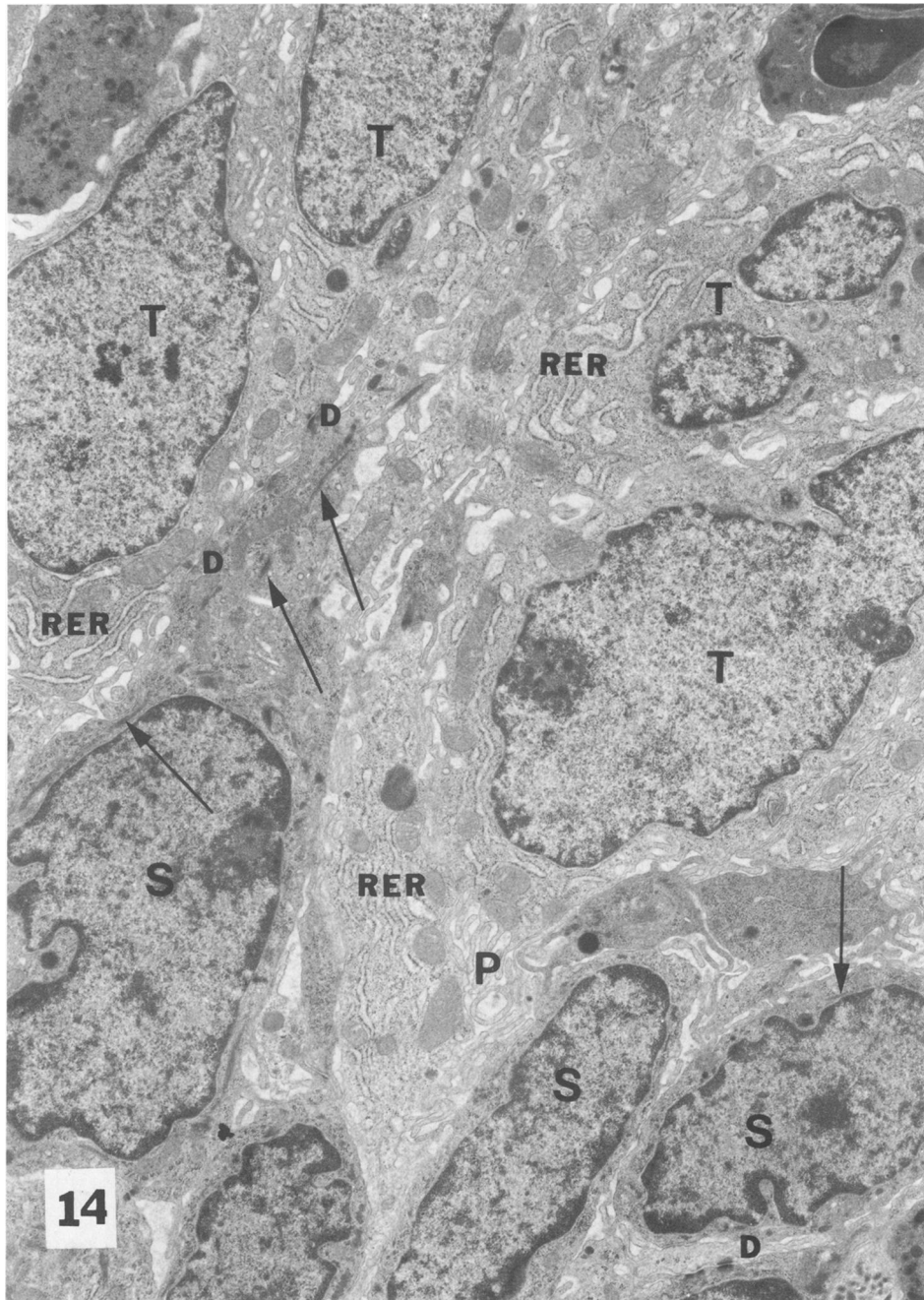
Figure 14—Poorly differentiated squamous cells (S) reveal electron-dense cytoplasm, scanty tonofibrils (arrows), and markedly interdigitated cytoplasmic processes (P) with a few desmosomes (D). The transitional cells (T) have electron-lucent cytoplasm showing scanty cellular organelles, parallel RER, dilatated RER cisternae with electron-dense granules, and interdigitated cytoplasmic processes. (× 7800)

sidered to be altered mature goblet cells rather than the basal cells.[33] Similar intermediate cells were described in the biopsy specimens and primary culture of poorly differentiated carcinomas of the human uterine cervix.[32] The studies of squamous metaplasia and carcinoma of tracheobroncheal epithelium in humans and hamsters described the intermediate cells and postulated that the squamous metaplasia occurred

by direct transformation of differentiated adult mucus cells to adult squamous cells.[34]

The generally prevailing concept is that the metaplastic cells are derived from a new type of differentiation of undifferentiated basal or reserve cells, rather than direct transformation of an adult columnar cell into an adult squamous cell.[35-40] The nasal epithelium was subjected to continuous remodeling by destruc-
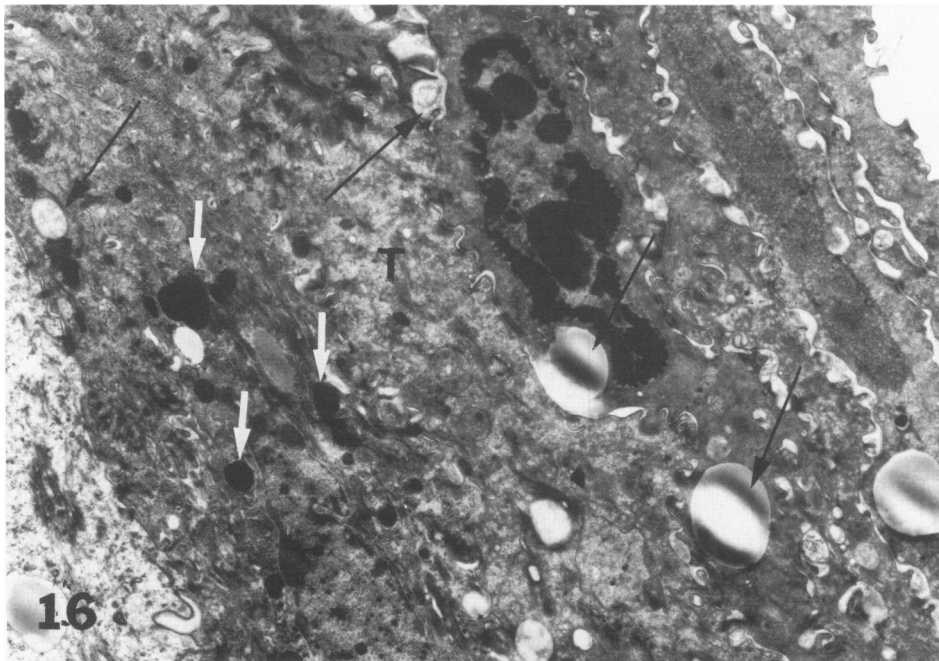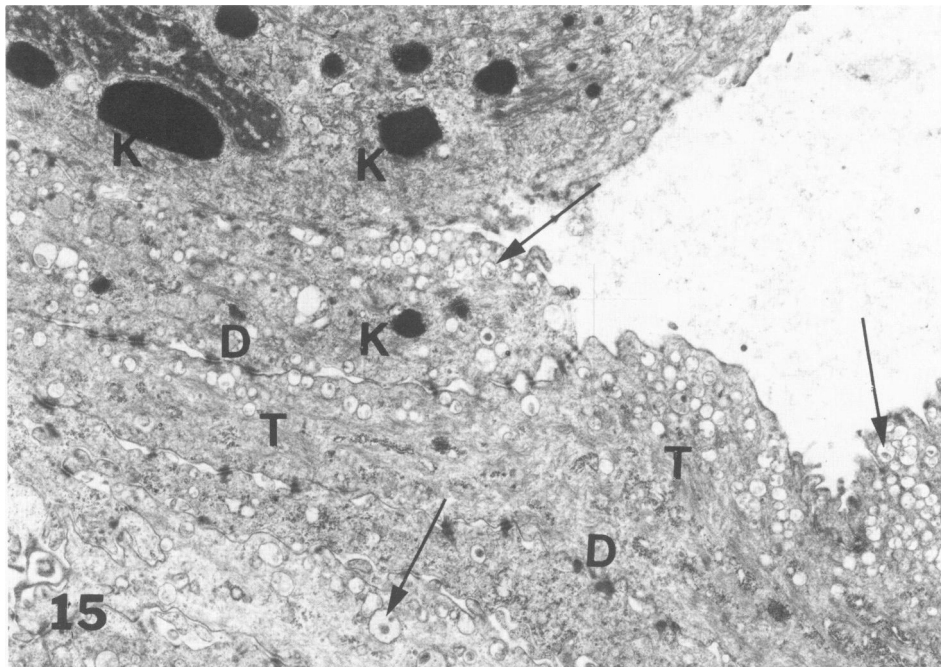
Figure 15—Notice the numerous aggregates of secretory vesicles (*arrows*) in the flattened squamous cells, showing tonofibrils (*T*), keratohyaline granules (*K*), and numerous well-developed desmosomes (*D*). (× 7800)   Figure 16—Keratocytes and keratin plates show numerous secretory droplets (*slender arrows*), keratohyaline granules (*white arrows*), and tonofibrils (*T*). (× 7800)

tion and repairing processes during HMPA exposure. The damaged respiratory epithelium was repaired initially by undifferentiated mucus cells and microvillous cuboidal cells. Subsequently, the superficial cells were replaced with squamous cell migration from the basal layer. In the early stage of squamous metaplasia, the epithelium was thickened by stratification of undifferentiated glandular cells, transitional cells, poorly differentiated squamous cells, and intermediate cells. Since the transitional cells are closely associated and resemble the undifferentiated glandular cells, the transitional cells, apparently derived from the undifferentiated glandular cells, differentiate to squamous cells. The undifferentiated glandular cells

seem to be biphasic reserve cells that can differentiate to either glandular or squamous cells. The intermediate cells, showing features of both glandular and squamous differentiation, appear to be developed from the undifferentiated glandular cells rather than direct transformation of adult goblet cells to adult squamous cells. The intermediate cells appeared with undifferentiated glandular cells in the basal layer when mature goblet cells in the superficial epithelium were denuded following HMPA exposure. Mitotic activity was observed in the basal cells and poorly differentiated squamous cells but not in the goblet or ciliated cells. The observation indicates that the necrotic mucus or ciliated cells can be repaired only by cellular differentiation from the reserve cells. There was no clear-cut evidence indicating the direct transformation of the adult mucus to squamous cells at the damaged superficial epithelium.

In the rats exposed to HMPA, the morphologic characteristics of the squamous metaplasia associated with squamous cell carcinoma were indistinguishable from squamous metaplasia not associated with squamous cancer. It was also difficult to distinguish the squamous cells of squamous metaplasia from those of well-differentiated squamous carcinoma. Both squamous cells in the squamous carcinoma and undifferentiated squamous cells in the squamous metaplasia showed poorly developed desmosomes, tonofibrils, cytoplasmic processes, and glycogen particulates. However, some squamous cells of the squamous carcinoma had prominent nuclear atypia. In addition, a greater number of intermediate cells, mucus droplets in the keratin plates, and intracellular or extracellular lumen showing microvillous or squamous luminal cells with desquamated cells and cellular debris was seen in the squamous carcinomas than in squamous metaplasia.[43] Nuclear atypia was described in the squamous metaplasia of tracheal epithelium produced by a chemical carcinogen[36] and mechanical injury.[41] In the squamous metaplasia of tracheal epithelium exposed to a chemical carcinogen, the epithelial cells showed an increased secretory activity and decreased desmosomes. Carcinoma *in situ* was characterized by numerous intracellular and extracellular microcysts with secretory material. Microinvasive carcinoma revealed secretory activity with nuclear atypia and laminated ergastroplasm.[44]

References

1. NIOSH (National Institute for Occupational Safety and Health): Background Information on Hexamethylphosphoric Triamide, US Department of Health, Education and Welfare, Rockville, Maryland, October 24, 1975
2. Chang SC, Terry PH, Borkovec AB: Insect chemosterilants with low toxicity for mammals. Science 1964, 144:57-58
3. Jackson H, Craig AW: Antifertility action and metabolism of hexamethylphosphoramide. Nature (London) 1966, 212:86-87
4. Jackson H, Davies P, Bock M: Chemosterilization of *Schistosoma mansoni*. Nature (London) 1968, 218:977
5. LaBrecque GC, Meifert DW: Control of house flies (Diptera: Musidae) in poultry houses with chemosterilants. J Med Entomol 1966, 3:323-326
6. Shott LD, Borkovec AB, Knapp WA, Jr: Toxicology of hexamethylphosphoric triamide in rats and rabbits. Toxicol Appl Pharmacol 1971, 18:499-506
7. Kimbrough RD, Sedlak VA: Lung morphology in rats treated with hexamethylphosphoramide. Toxicol Appl Pharmacol 1968, 12:60-67
8. Jackson H, Jones AR, Cooper ERA: Effects of hexamethylphosphoramide on rat spermatogenesis and fertility. J Reprod Fertil 1969, 20:263-269
9. Overcash RG, Lindsey JR, Cassell GH, Baker HJ: Enhancement of natural and experimental respiratory mycoplasmosis in rats by hexamethylphosphoramide. Am J Pathol 1976, 82:171-186
10. Zapp JA: HMPA: A possible carcinogen. Science 1975, 190:422
11. Lee KP, Trochimowicz HJ: Induction of nasal tumors in rats exposed to hexamethylphosphoramide (HMPA) by inhalation. J Natl Cancer Inst (In press)
12. Mosbech J, Acheson ED: Nasal cancer in furniture makers in Denmark. Dan Med Bull 1971, 19:34-35
13. Formbeur JP: Recent cases of ethmoid-maxillary tumors in wood-workers. Arch Mal Prof Med Trav Secur Soc 1972, 33:453-455
14. Hadfield EH: Cancer hazard from wood dust and in the boot and shoe industry. Ann Occup Hyg 1972, 15:39-41
15. Acheson EO: Nasal cancer in the furniture and boot and shoe manufacturing industries. Prev Med 1976, 5:295-315
16. Konetzke GW: The carcinogenic action of arsenic and nickel. Arch Geschwulstforsch 1974, 44:16-22
17. Pedersen E, Hogetviet AC, Andersen A: Cancer of respiratory organs among workers at a nickel refinery in Norway. Int J Cancer 1973, 12:32-41
18. Swenberg JA, Kerns WD, Mitchell RI, Gralla EJ, Pavkov KL: Induction of squamous cell carcinomas of the rats nasal cavity by inhalation exposure to formaldehyde vapor. Cancer Res 1980, 40:3398-3401
19. Kuschner M, Laskin S, Drew RT, Cappiello V, Nelson N: Inhalation carcinogenicity of alpha helo ethers: III. Lifetime and limited period inhalation studies with bis(chloromethyl) ether at 0.1 ppm. Arch Environ Health 1975, 30:733-77
20. Laskin S, Drew RT, Cappiello V, Kuschner M, Nelson N: Inhalation carcinogenicity of alpha helo ethers: II. Chronic inhalation studies with chloromethyl ether. Arch Environ Health 1975, 30:70-72
21. Chemical Regulation Reporter: Phenylglycidyl ether. 31:1336, 1979
22. Chemical Regulation Reporter: Dichlorobutene. 3: 1324, 1979
23. NIOSH Current Intelligence: Dimethylcarbamoyl chloride. Bulletin No. 11, July 1976
24. NIOSH Current Intelligence: Epichlorohydrin. Bulletin No. 30, 1978
25. Reznik-Schüller H, Mohr U: Ultrastructure of N-Nitrosodibutylamine-induced tumors of the nasal

cavity in the European hamster. J Natl Cancer Inst 1976, 57:401-407

26. Black H, Akerman LV: The importance of epidermoid carcinoma in situ in the histogenesis of carcinoma of the lung. Ann Surg 1952, 136:44-45

27. Becci PJ, McDowell EM, Trump BF: The respiratory epithelium: IV. Histogenesis of epidermoid metaplasia and carcinoma in situ in the hamster. J Natl Cancer Inst 1978, 61:577-586

28. Martin SW, Willoughby RA: Organic dusts, sulfur dioxide, and the respiratory tract of swine. Arch Environ Health 1972, 25:158-165

29. Klacemann PG, Olson JL, Eggleston JC: Mucoepidermoid carcinoma of the bronchus: An electron microscopic study of the low grade and the high grade variants. Cancer 1979, 43:1720-1733

30. Mullins JO, Barnes RP: Childhood bronchial mucoepidermoid tumors: A case report and review of the literature. Cancer 1979, 43:315-322

31. Tomita T, Lotuaco L, Talbott L, Watanabe I: Mucoepidermoid carcinoma of the subglottes: An ultrastructural study. Arch Pathol Lab Med 1977, 101:145-148

32. Aversperg N, Erher H: Effects of tissue culture environment on growth patterns and ultrastructure of poorly differentiated humans cervical carcinomas. J Natl Cancer Inst 1976, 57:981-993

33. Wang N-S, Huong S-N, Thurlbeck WM: Squamous metaplasia of the opening of bronchial glands. Am J Pathol 1972, 67:571-582

34. Trump BF, McDowell EM, Galvin F, Barrett LA, Becci PJ, Schürch W, Kaiser HE: The respiratory epithelium: III. Histogenesis of epidermoid metaplasia and carcinoma in situ in the human. J Natl Cancer Inst 1978, 61:563-575

35. Harris CC, Kaufman DG, Sporn MB, Smith JM, Jackson FE, Saffioti U: Ultrastructural effects of N-methyl-N-nitrosourea on the tracheobronchial epithelium of the Syrian golden hamster. Int J Cancer 1973, 12:259-269

36. Harris CC, Sporn MB, Kaufman DG, Smith JM, Jackson FE, Saffioti U: Histogenesis of squamous metaplasia in the hamster tracheal epithelium caused by vitamin A deficiency of benzo[a]pyrene-ferric oxide. J Natl Cancer Inst 1972, 48:743-761

37. Harris CC, Kaufman DG, Sporn MB, et al: Histogenesis of squamous metaplasia and squamous cell carcinoma of the respiratory epithelium in an animal model. Cancer Chemother Rep (Suppl) 1973, 4:43-54

38. Niskanen KO: Observations on metaplasia of bronchial epithelium and its relation to carcinoma of lung: Patho-anatomical and experimental researches. Acta Pathol Microbiol Scand 1949, 80(Suppl)80:1-80

39. Stenback F: Morphologic characteristics of experimentally induced lung tumors and their precursors in hamsters. Acta Cytol (Baltimore) 1973, 17:476-486

40. Asmundsson T, Kilburn KH, McKenzie WN: Injury and metaplasia of airway cells due to SO_2. Lab Invest 1973, 19:41-53

41. McDowell EM, Becci PJ, Schürch W, Tramp BF: The respiratory epithelium: VII. Epidermoid metaplasia of hamster tracheal epithelium during regeneration following mechanical injury. J Natl Cancer Inst 1979, 62:995-1001

42. Becci PJ, McDowell EM, Trumph BF: The respiratory epithelium: IV. Histogenesis of lung tumors induced by benzo[a]pyrene-ferric oxide in the hamster. J Natl Cancer Inst 1978, 61:607-618

43. Lee KP, Trochimowicz HJ: Ultrastructure of nasal tumors in the rats exposed to hexamethylphosphoramide (HMPA) by inhalation. Cancer Res (In press)

44. Klein-Szanto AJP, Topping DC, Heckman CA, Nettesheim P: Ultrastructural characteristics of carcinogen-induced nondysplastic changes in tracheal epithelium. Am J Pathol 1979, 98:61-82

Acknowledgments